Materials Science-Poland, Vol. 24, No. 1, 2006

Structural and transport properties of $LiFe_{0.45}Mn_{0.55}PO_4$ as a cathode material in Li-ion batteries

W. OJCZYK[1], J. MARZEC[1], J. DYGAS[2], F. KROK[2], R. S. LIU[3], J. MOLENDA[1*]

[1]Faculty of Materials Science and Ceramics, AGH University of Science and Technology, al. Mickiewicza 30, 30-059 Cracow, Poland

[2]Faculty of Physics, Warsaw University of Technology, pl. Politechniki 1, 00-661 Warsaw, Poland

[3]Department of Chemistry, National Taiwan University, Roosevelt Road, Taipei 106, Taiwan, R.O.C.

The paper presents investigations on structural, electrical and electrochemical properties of phospho-olivine, $LiFe_{0.45}Mn_{0.55}PO_4$, synthesized at high temperatures. Moessbauer spectroscopy measurements confirmed the occurrence of iron(II), and X-ray absorption near edge structure (XANES) measurements evidenced manganese(II) and iron(II). Impedance spectroscopy enabled the separation of electrical conductivity into electronic and ionic components. The substitution of manganese for iron led to a noticeable increase in the electronic component of conductivity and only to a slight increase in the ionic component, compared to pure $LiFePO_4$. Also, the chemical diffusion coefficient of lithium measured by GITT turned out larger in $Li_xFe_{0.45}Mn_{0.55}PO_4$. It has been stated that the increased electronic conductivity in manganese-doped phospho-olivine activates the diffusional mechanism of lithium deintercalation.

Key words: *$LiMn_yFe_{1-y}PO_4$; lithium diffusion; cathode material; Li-ion battery; intercalation*

1. Introduction

In the large group of compounds that can reversibly react with lithium, phosphates in particular draw the attention of researchers [1, 2]. The most promising ones are phosphates with a general formula of $LiMPO_4$ (M = Fe, Mn, Co, Ni) and the olivine structure. $LiFePO_4$ is characterized by high voltage (3.5 V) and capacity (170 mA·h/g), outstanding chemical stability, low cost, and environmental friendliness. The electrochemical charging of a $Li \mid Li^+ \mid LiFePO_4$ cell yields a two-phase product, according to the following equation:

*Corresponding author, e-mail: molenda@uci.agh.edu.pl

$$Li_{1-x}FePO_4 - xLi^+ - xe^- \rightarrow xFePO_4 + (1-x)LiFePO_4 \quad (1)$$

Yamada et al. [3–5] reported that the chemical delithiation of phospho-olivine, $LiMn_{0.6}Fe_{0.4}PO_4$, at a voltage of 3.5V, proceeds as follows:

$$LiFe_{1-y}Mn_yPO_4 - xLi^+ - xe^- \rightarrow Li_{1-x}Fe_{1-y}Mn_yPO_4 \quad (0 < 1-x < y) \quad (2)$$

This voltage accounts for the oxidation of iron, $Fe^{2+} \rightarrow Fe^{3+}$. At 4 V, where manganese oxidation takes place ($Mn^{2+} \rightarrow Mn^{3+}$) the mechanism of reaction changes and a two-phase product is obtained according to the reaction [3–5]:

$$Li_yFe_{1-y}Mn_yPO_4 - xLi^+ - xe^- \rightarrow x/y\ Fe_{1-y}Mn_yPO_4 + (y-x)/y\ Li_yFe_{1-y}Mn_yPO_4 \quad (3)$$

The goal of this work was to investigate structural, electrical, and electrochemical properties of manganese-doped phospho-olivine, $LiFe_{0.45}Mn_{0.55}PO_4$, and the properties of this compound after electrochemical deintercalation in a $Li \mid Li^+ \mid LiFe_{0.45}Mn_{0.55}PO_4$ cell in order to asses the delithiation mechanism.

2. Experimental details

$LiFe_{0.45}Mn_{0.55}PO_4$ and $LiFePO_4$ olivines were synthesized by a high temperature reaction using Li_2CO_3 (POCh, pure p.a.), $MnCO_3$ (Aldrich, pure p.a.), $FeC_2O_4 \cdot 2H_2O$ (Aldrich, pure), and $NH_4H_2PO_4$ (POCh, pure p.a.). The substances were thoroughly ground in an agate mortar with some acetone added, then dried and pressed into pellets. Initial heating and synthesis were performed under argon of high purity, with the following sequence of time/temperature regimes: 1.5 h at 100 ºC (to remove water from the system), 2h at 260 ºC (to decompose iron oxalate), 3h at 350 ºC (to remove gaseous products and initiate the synthesis). The final heating was performed at 750 ºC for 24 h. This complex procedure was developed in order to avoid the oxidation of Fe^{2+} and to minimize the formation of phosphides and $Mn_yFe_{1-y}P_2O_7$ [6]. The colour of the samples varied from dark grey for samples with high iron content to light grey for samples with 55 at. % of manganese.

In the electrochemical studies, composite cathodes were used containing 85 wt. % of $LiFe_{0.45}Mn_{0.55}PO_4$, 7.5 wt. % graphite, and 7.5 wt. % of carbon obtained from the decomposition of a phenol-formaldehyde resin. The additives, being electronic conductors, were necessary because of the high resistivity of the samples ($> 10^9\ \Omega \cdot cm$). The additives constituted a highly conductive matrix, in which the much less conductive olivine dispersions were imbedded. This microstructure allowed the olivine capacity to be taken advantage of [7–9].

The samples were characterized by XRD (Phillips X'Pert Pro), SEM (JEOL JSM 5400), and EDS. The X-ray spectra were analysed using the Rietveld method. Iron oxidation state and its local surroundings were characterized by ^{57}Fe Moessbauer spectroscopy at 300 K, with the spectrometer operating in constant acceleration mode

in transmission geometry and with a ^{57}Co(Rh) source. The oxidation states of Fe and Mn were also characterized by X-ray absorption near edge structure (XANES) measurements. XANES was carried out at the Wiggler beam line BL 17C of National Synchrotron Radiation Research Center (NSRRC), Taiwan. The electron storage ring was operated at the energy of 1.5 GeV with a beam current of 100–200 mA. A Si(111) double-crystal monochromator was employed for energy selection, with a resolution ($\Delta E/E$) of ca. 2×10^{-4}. The XANES spectra at the Fe and Mn K-edges were recorded at room temperature in a transmission mode, using gas-filled ionisation chambers to measure the intensities of the incident and transmitted X-ray spectra, which were normalized with respect to edge jump.

The specimens for impedance spectroscopy measurements were shaped into flat pellets, ground with abrasive papers of up to 2400 grit No. Electrodes were made of thin layers of gold deposited on flat surfaces of the pellets by plasma spraying. Thus prepared specimens were inserted between two mounting plates in a spring holder. Measurements were performed in flowing argon, purity N5. The impedance was recorded with a laboratory set-up comprising a Solartron 1260 analyser and Keithley 428 current amplifier operating in the frequency range 10^{-2}–10^{7} Hz with an alternating voltage excitation (rms value of 30 mV). The specimens were thermostated by means of an electric furnace with a constant voltage supply. Measurements within the temperature range 300–600 K were repeated in each case when the measuring algorithm detected impedance drift during 30 min of data acquisition (spectrum consisting of 160 frequencies).

The electrochemical extraction of lithium was performed in $Li\,|\,Li^+\,|\,Li_{1-x}Fe_{0.45}Mn_{0.55}PO_4$ cells using a lithium metal anode, Selectipur LP71 electrolyte (EC:DEC:DMC 1:1:1, 1 M $LiPF_6$, Merck), and a composite cathode, as described above. The charging curves of the cells, OCV, and lithium diffusion coefficient were determined as a function of lithium concentration in the cathode material. Lithium diffusion was measured by GITT (Galvanostatic Intermittent Titration Technique), as described by Weppner and Huggins [10], with a current impulse of 300 $\mu A/cm^2$ lasting 130 s.

3. Results and discussion

According to the X-ray analyses, the $LiFe_{0.45}Mn_{0.55}PO_4$ material, synthesized at high temperatures, is single-phase and has the olivine structure (space group *Pnma*) (Fig. 1). Its X-ray spectrum is shown in Fig. 2. Lattice constants were determined by the Rietveld method. An example of the specimen's microstructure is given in the SEM micrograph in Fig. 3a. The size of agglomerates is 10–50 μm, and they are built of crystallites about 1 μm long. The distribution of elements over the grain surface was analysed by EDS (Fig. 3b). The analysis was taken at different points within the same grains, and showed a homogeneous distribution of elements and absence of im-

purities such as iron or manganese phosphides and carbophosphides [11]. The EDS spectrum of $LiFe_{0.45}Mn_{0.55}PO_4$ confirmed the assumed iron-to-manganese ratio. The small amount of carbon detected locally originates from the decomposition of the starting reagents.

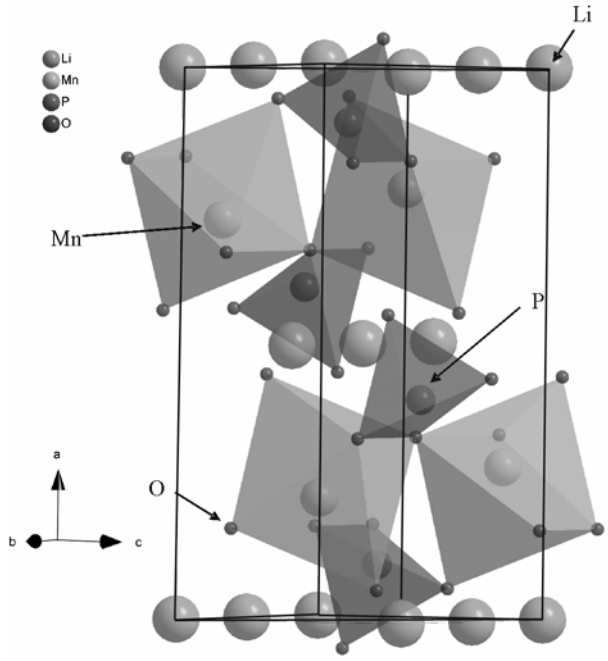

Fig. 1. The olivine structure of $LiMnPO_4$

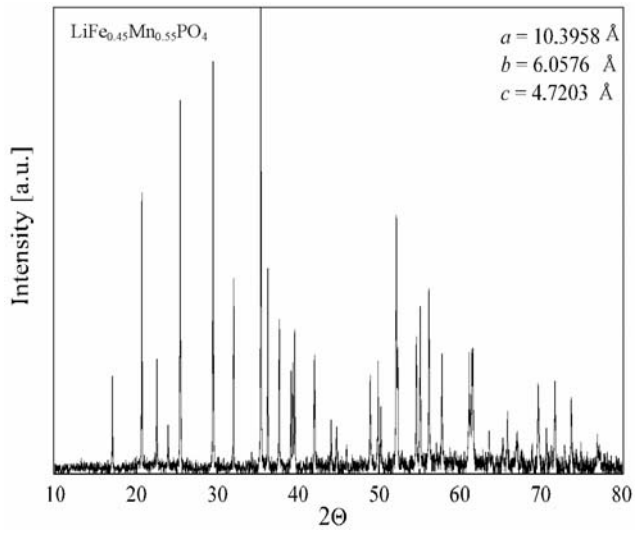

Fig. 2. X-ray diffraction pattern of $LiFe_{0.45}Mn_{0.55}PO_4$

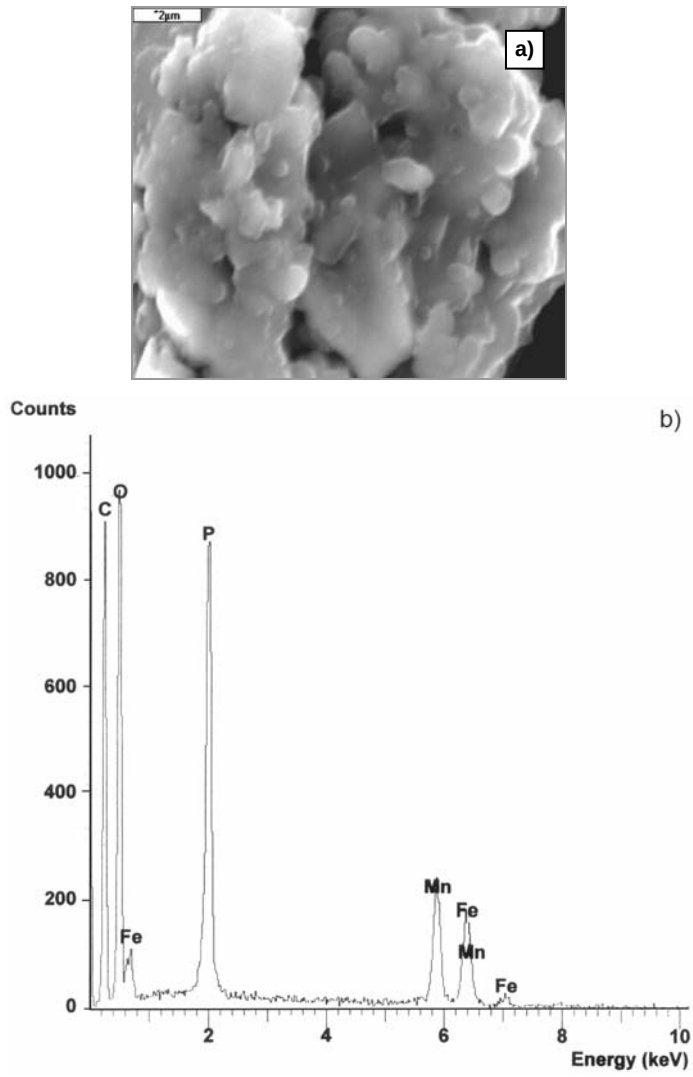

Fig. 3. Powder microstructure of $LiFe_{0.45}Mn_{0.55}PO_4$ (a) and its point EDS spectra (b)

The results of Moessbauer spectroscopy studies are presented in Fig. 4. The quadrupole doublet indicates iron(II) atoms in one crystallographic site. The oxidation numbers of manganese and iron could be determined by means of XANES (Fig. 5a, b). At different compositions of $LiFe_{1-y}Mn_yPO_4$ (y = 0, 0.25, 0.55, 0.75), the oxidation numbers of both these elements were always 2+. A detailed description of the determination mode of the oxidation state for Fe in $LiFePO_4$ has been published by Prince et al. [12]. These results indicate that the synthesis route followed in this work prevents the appearance of impurities containing Fe^{3+} [5].

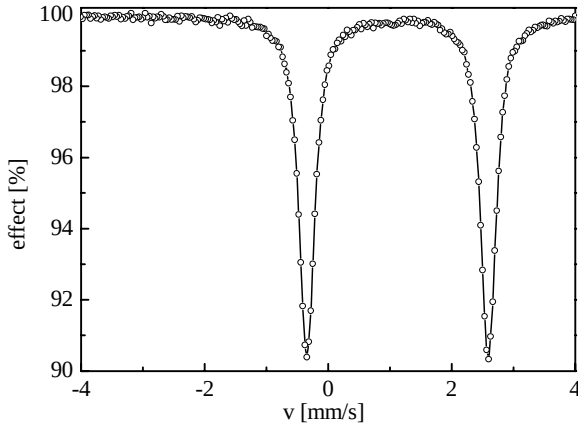

Fig. 4. Moessbauer spectrum of the $Li_1Fe_{0.45}Mn_{0.55}PO_4$ cathode material

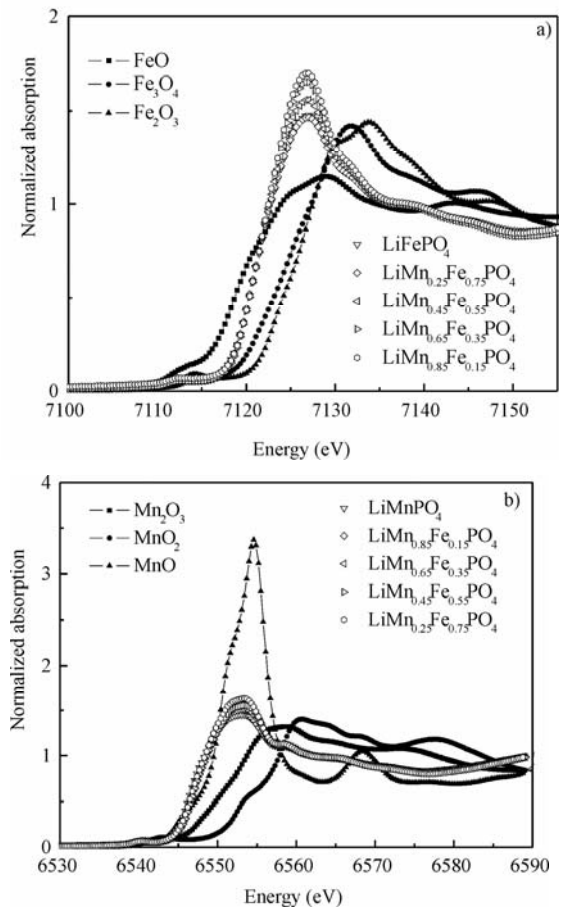

Fig. 5. The Fe K-edge (a) and Mn K-edge XANES spectra (b) of $LiFe_{1-y}Mn_yPO_4$ (y = 0, 0.25, 0.55, 0.75)

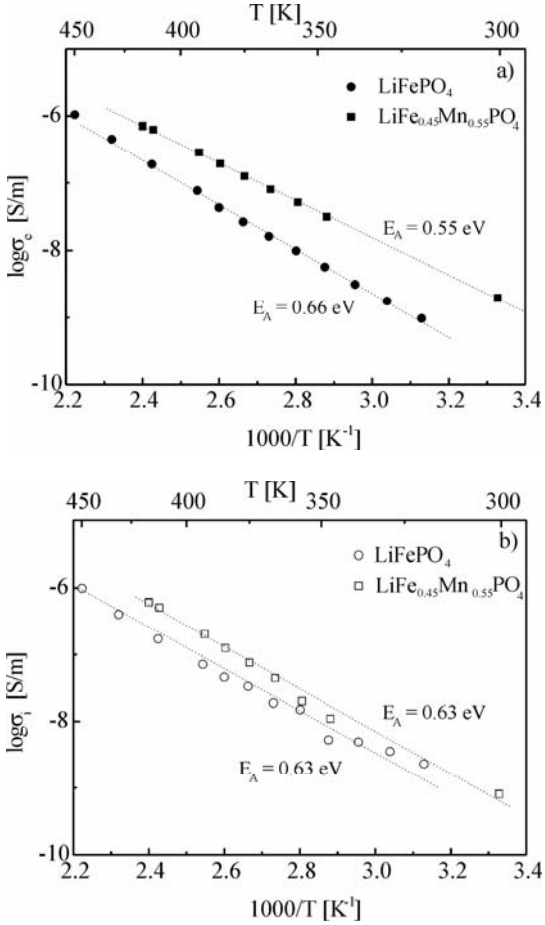

Fig. 6. The temperature dependences of the electronic (a) and ionic (b) conductivities of $LiFePO_4$ and $LiFe_{0.45}Mn_{0.55}PO_4$

The temperature dependences of the electronic and ionic conductivities of $LiFePO_4$ and $LiFe_{0.45}Mn_{0.55}PO_4$ are shown in Fig. 6a and b. The electronic conductivity of iron-manganese phospho-olivine is one order of magnitude higher than that of undoped $LiFePO_4$. The activation energies of electronic conductivities for $LiFe_{0.45}Mn_{0.55}PO_4$ and $LiFePO_4$ are 0.55 eV and 0.66 eV, respectively. The lower activation energy of electronic conductivity for the iron-manganese phospho-olivine is related to the presence of Fe^{2+}–Mn^{2+} pairs. The electronic configuration of manganese(II) is $3d^5$, while that of iron(II) is $3d^6$, which facilitates charge transport between these two types of ions. Structural relationships in phospho-olivine (Fig. 1) seem to favour charge transport via Fe–O–Mn bonds, where the interionic distance between Mn^{2+} and Fe^{2+} is about 4 Å. The lower electronic conductivity of $LiFePO_4$ is related to the presence of only one type of transition metal ion, namely Fe^{2+} ($3d^6$). The room-temperature ionic conductivities of both compounds are similar, a slightly higher value, however, has been

recorded for iron-manganese phospho-olivine. The activation energies of ionic conductivities have the same value for pure and manganese-doped phospho-olivine and close to the values calculated by numerical methods [13, 14]. In spite of increasing electronic conductivity, the ionic conductivity of $LiFe_{0.45}Mn_{0.55}PO_4$ remains practically unchanged. This may indicate that one-dimensional diffusion paths in the olivine structure are insufficient for fast lithium transport.

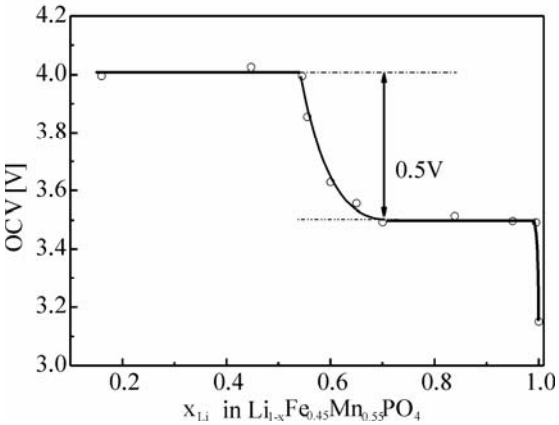

Fig. 7. OCV curve for a $Li\,|\,Li^+\,|\,Li_{1-x}Fe_{0.45}Mn_{0.55}PO_4$ cell as a function of lithium concentration

Figure 7 presents the OCV curve of the $Li\,|\,Li^+\,|\,Li_{1-x}Fe_{0.45}Mn_{0.55}PO_4$ cell with two characteristic plateaus. The first one, at 3.5V versus the lithium electrode, is related to iron oxidation ($Fe^{2+} \rightarrow Fe^{3+}$), and the second one at 4 V to manganese oxidation ($Mn^{2+} \rightarrow Mn^{3+}$). The sudden change in voltage by about 0.5 V is observed at $x_{Li} = 0.45$. In the composition range where the voltage is equal to 3.5 V and iron oxidation takes place, a linear variation of the lattice parameters of phospho-olivine with lithium content is observed. The lattice constants of $Li_{1-x}Fe_{0.45}Mn_{0.55}PO_4$, calculated by the Rietveld method, are given in Figure 8. The *a*, *b*, *c* lattice constants change linearly as lithium deintercalation proceeds, up to $x_{Li} = 0.45$. When lithium concentration becomes lower than 0.45, the X-ray spectrum indicates a single-phase material but the lattice parameters remain constant. It seems that such a behaviour can be explained on the basis of some earlier studies [15]. It has been stated that during lithium deintercalation at the voltage of 4 V, phospho-olivine phases with different lithium concentrations are formed. This observation seems to be in accordance with the model developed by Andersson [16], according to which the delithiation of phospho-olivines does not proceed in a radial mode, but by a mosaic mode, involving the appearance of microregions with and without lithium in the cathode material. Yamada [3–5] has shown that lithium deintercalation is a diffusional process at 3.5 V, while at 4 V manganese oxidation ($Mn^{2+} \rightarrow Mn^{3+}$) leads to the formation of two phases (Eq. (3)). The different delithiation mechanisms of phospho-olivine, observed by the authors at 4 V,

may be related to the fact that in Yamada's experiments lithium was extracted chemically in NO_2BF_4 solution. It has been demonstrated earlier [17] that the electrochemical and chemical deintercalation of lithium from manganese spinel yields products with different physical and chemical properties.

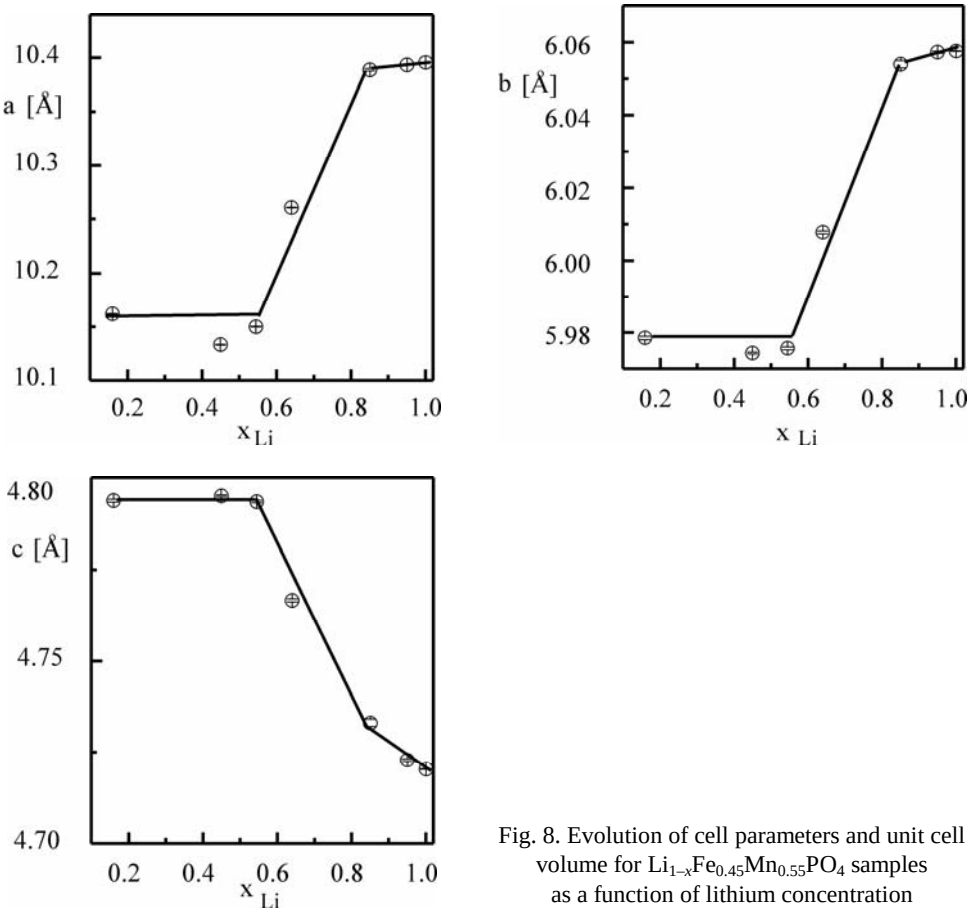

Fig. 8. Evolution of cell parameters and unit cell volume for $Li_{1-x}Fe_{0.45}Mn_{0.55}PO_4$ samples as a function of lithium concentration

Figure 9 presents the chemical diffusion coefficient of lithium as a function of lithium concentration in the cathode material, with a maximum of D_{Li} at $x_{Li} = 0.45$. The significant increase (about two orders of magnitude) in the diffusion coefficient can be related to the increased number of sites available for lithium diffusion in the $Li_{1-x}Fe_{0.45}Mn_{0.55}PO_4$ structure. At a lower concentration of lithium, the chemical diffusion coefficient D_{Li} decreases, which reflects some change in the relaxation mechanism of the cathode material. Despite the slight improvement in electronic conductivity, the chemical diffusion coefficient of lithium in $LiFe_{0.45}Mn_{0.55}PO_4$ remains low and increases only at a lithium concentration of about 0.45. The observed diffusion coefficients do not exceed $10^{-11}cm^2/s$, and are about 3–5 orders of magnitude lower than in the case of $LiMn_2O_4$ [18] or $LiNi_{1-y}Co_yO_2$ [19]. This may indicate that not only the

crystallographic structure, but also low electronic conductivity limits the effectiveness of $LiFe_{0.45}Mn_{0.55}PO_4$ in the electrode process.

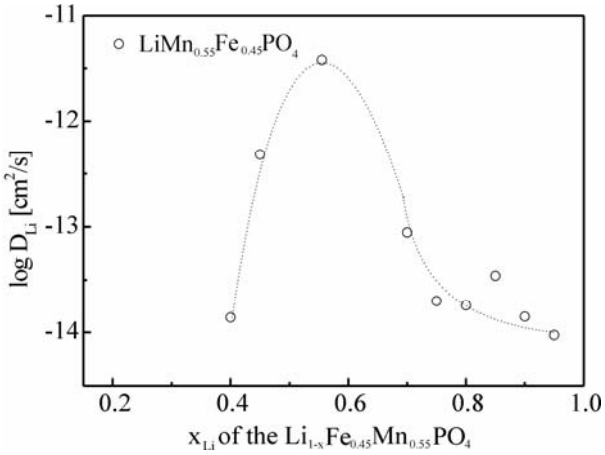

Fig. 9. Effective diffusion coefficient of lithium measured in a $Li\,|\,Li^+\,|\,Li_{1-x}Fe_{0.45}Mn_{0.55}PO_4$ cell. The line serves as a guide for the eyes

It seems that the one-dimensional diffusion paths, which can be easily blocked, disable fast lithium migration in this material. The phenomenon of cation mixing may additionally decrease the effective diffusion of lithium. A 3d metal substituted for lithium in the olivine structure blocks the diffusion path. It seems that a better effectiveness of the cathode process in the case of olivines ($LiFe_{1-y}Mn_yPO_4$) might be attained by microstructure optimisation, e.g. by using nanopowders with high specific surfaces.

4. Conclusions

Impedance spectroscopy studies of electrical conductivity in the temperature range 300–460 K have shown an increased electronic conductivity of $LiFe_{1-y}Mn_yPO_4$ as compared to $LiFePO_4$, while the ionic conductivity and chemical diffusion coefficient of lithium were only slightly higher than those of $LiFePO_4$. It seems that the increased electronic conductivity activates the diffusional mechanism of deintercalation, whereas it does not change the chemical diffusion coefficient of lithium to any significant degree.

Acknowledgement

This work was supported by the State Committee for Scientific Research, Poland under grant No. 4 T08A 020 25.

References

[1] PADLI A.K., NANJUNDASWAMY K.S., GOODENOUGH J.B., J. Electrochem. Soc., 144 (1997), 1188.
[2] PADLI A.K., NANJUNDASWAMY K.S., MASQUELIER C., OKADA S., GOODENOUGH J.B., J. Electrochem. Soc., 144 (1997), 1609.
[3] YAMADA A., KUDO Y., LIU K.-Y., J. Electrochem. Soc., 148 (2001), A747.
[4] YAMADA A., KUDO Y., LIU K.-Y., J. Electrochem. Soc., 148 (2001), A1153.
[5] YAMADA A., KUDO Y., CHUNG. S.CH., J. Electrochem. Soc., 148 (2001), A960.
[6] HONG Y.-S., RYU K.S., PARK Y.J., KIM M.G., LEE J.M., CHANG S.H., J. Mater. Chem., 12 (2002), 1870.
[7] OKADA S., SAWA S., EGASHIRA M., YAMAKI J.I., TABUCHI M., KAGEYAMA H., KONISHA T., YOSHINO A., J. Power Sources, 97–98 (2001), 430.
[8] YAMADA A., HOSOYA M., CHUNG. S.CH., KUDO Y., HINOKUMA K., LIU K.-Y., NISHI Y., J. Power Sources, 119–121 (2003), 232.
[9] FRANGER S., LE CARS F., BOURBON C., ROUAULT H., J. Power Sources, 119–121 (2003), 252.
[10] WEPPNER W., HUGGINS R.A., J. Electrochem. Soc., 124, (1977), 1569.
[11] HERLE S., ELLIS B., COOMBS N., NAZAR L.F., Nature Materials, **2** (2004), 147.
[12] PRINCE A.A.M., MYLSWAMY S., CHAN T.S., LIU R.S., HANNOYER B., JEAN M., SHEN C.H., HAUNG S.M., LEE J.F., WANG G.X., Solid State Commun., 132 (2004), 455.
[13] MORGAN D., VAN DER VEN A., CEDER G., Electrochem. Solid State Lett., 7 (2004), A30.
[14] RISSOULI K., BENKHOUJA K., RAMOS-BARRADO J.R., JULIEN C., Mater. Sci. Eng., B98 (2003), 185.
[15] OJCZYK W, MARZEC J., ŚWIERCZEK K., MOLENDA J., Defect Diffusion Forum, 237–240 (2005), 1299.
[16] ANDERSSON A.S., THOMAS O.J., J. Power Sources, 97–98 (2001), 498.
[17] MOLENDA J., OJCZYK W, MARZEC M., MARZEC J., PRZEWOŹNIK J., DZIEMBAJ R., MOLENDA M., Solid State Ionics, 157 (2003), 73.
[18] MOLENDA J., ŚWIERCZEK K., MOLENDA M., MARZEC J., Solid State Ionics, 135 (2000), 53.
[19] MOLENDA J., WILK P., MARZEC J., Solid State Ionics, 157 (2003), 115.

Received 10 December 2004
Revised 18 March 2005